

Target dependence of clan model parameter in $^{84}\text{Kr}_{36}$ – Emulsion interactions at 1 GeV per nucleon

M K SINGH^{1,2,3}, A K SOMA³, V SINGH^{1,3,*} and R PATHAK²

¹Physics Department, Banaras Hindu University, Varanasi 221 005, India

²Physics Department, Tilak Dhari Postgraduate College, Jaunpur 222 002, India

³Institute of Physics, Academia Sinica, Taipei 11529, Taiwan

*Corresponding author. E-mail: venkaz@yahoo.com

MS received 16 July 2013; revised 1 January 2014; accepted 28 January 2014

DOI: 10.1007/s12043-014-0779-5; ePublication: 28 August 2014

Abstract. This article focusses on the study of clan model parameters and their target dependence in light of void probability scaling for heavy (Ag and Br) and light (C, N and O) groups of target present in nuclear emulsion detector using $^{84}\text{Kr}_{36}$ at ~ 1 A GeV. The variation of scaled rapidity–gap (rap–gap) probability with single moment combination has been studied. We found that experimental points lie approximately on the negative binomial distribution (NBD) curve, indicating a scaling behaviour. The increase in average clan multiplicities (\bar{N}) for interactions with the pseudorapidity interval ($\Delta\eta$) was also observed. The values of \bar{N} for AgBr targets are larger than those for C/N/O target and also average number of particles per clan (\bar{n}_c) increases with increase in pseudorapidity interval. We further observed that for a particular target, the average number of particles per clan (\bar{n}_c) increases with an increase in the size of projectile nucleus.

Keywords. $^{84}\text{Kr}_{36}$ –emulsion interaction; nuclear emulsion detector; clan model parameters and their target dependence.

PACS Nos 29.40.Rg; 25.75.–q; 13.85.–t

1. Introduction

The search for quark gluon plasma (QGP) state in nucleon–nucleus or nucleus–nucleus interactions at high energy is one of the main objectives of relativistic heavy-ion experiments [1–6]. The multiplicity variable studies elucidate on a number of particles produced in interactions and thus quantify the physics behind multiparticle production process. Therefore, multiplicity parameter helps in testing phenomenological and theoretical models. The charged particle multiplicity distributions at various energies in hadron–hadron, hadron–nucleus and nucleus–nucleus interactions have attracted the attention of physicists for a long time [7]. Scientists conveyed several important observations and physics messages by studying the multiplicity distribution of produced or

emitted particles using a variety of projectile beams with a wide span of energy in recent times [7].

In a cascade event, any particle produced from a primary cluster is termed as ancestor and all the particles having common ancestor form a clan [7]. The clans have no mutual interactions, whereas the particles emitted due to disintegration of a clan have strong correlations. In the context of the clan model, average clan multiplicity \bar{N} and the average number of particles per clan \bar{n}_c are of immense physical importance and are referred to as clan model parameters [7–11]. The clan model parameter can be calculated by rapidity-gap (rap-gap) probability scaling, which is also known as void probability scaling [12]. The rap-gap probability is defined as the probability of events with zero particles in a specific region of phase-space [12–14]. In an earlier research, it was reported that rap-gap probability $P_0(\Delta\eta)$ is a useful parameter to study correlations among secondary particles produced in certain interactions [7–11].

The rap-gap probability $P_0(\Delta\eta)$ with a scaling behaviour was predicted by the hierarchical models in the central rapidity domains in high-energy nucleus–nucleus collisions, by many authors [7–12]. All the analyses provided sensitive tests for the linked-pair approximation of the higher-order cumulant correlations. However, only a few of them study the clan model parameters from void probability scaling in nucleus–nucleus interactions. In this paper, we have computed clan model parameters and studied their target dependence in light of void probability scaling in high-energy nucleus–nucleus interactions. For this study we used heavy (Ag/Br) and light (C/N/O) groups of target present in the nuclear emulsion. The projectile used for this study is $^{84}\text{Kr}_{36}$ at ~ 1 A GeV. In order to be certain about the void probability scaling, we have calculated the scaled rap-gap probability and shown its variation with the single moment combination for the interactions. The experimental points have been fitted separately with the negative binomial (NB) model and the minimal model. We have also compared our results with the results of [7–14].

2. Experimental details

Data used in this analysis were collected with a stack of highly sensitive NIKFI BR-2 nuclear emulsion plates of $9.8 \times 9.8 \times 0.06$ cm³ dimensions, which were exposed horizontally by $^{84}\text{Kr}_{36}$ ion of ~ 1 GeV kinetic energy per nucleon. The exposure was performed at Gesellschaft fur Schwerionenforschung (GSI) Darmstadt, Germany. Interactions were found by along-the-track scanning technique using an oil immersion objective of $100\times$ magnification. Two standard methods were used for scanning of the emulsion plates, one was the line scanning and other was the volume scanning. In line scanning method, beam tracks were picked up at a distance of 5 mm from the edge of the plate and were carefully followed until they either interacted with nuclear emulsion detector (NED) nuclei or escaped from any surface of emulsion. In volume scanning, emulsion plates were scanned strip by strip and event information was collected [6,15,16].

All secondary charged particles produced in an interaction are classified in accordance with ionization or normalized grain density (g^*), range (L) and velocity (β) into three categories [16–18].

2.1 Shower tracks (N_s)

These are freshly created charged particles with $g^* < 1.4$. These particles have $\beta > 0.7$. They are mostly fast pions with a small admixture of kaons and released protons from the projectile that have undergone an interaction. For the case of proton, kinetic energy (E_p) should be less than 400 MeV.

2.2 Grey tracks (N_g)

The particles with range $L > 3$ mm and $1.4 < g^* < 6.0$ are defined as greys. They have β in the range of $0.3 < \beta < 0.7$. These are generally knocked-out protons (NEDs cannot detect neutral particle) of targets with kinetic energy between 30 and 400 MeV, and traces of deuterons, tritons and slow mesons.

2.3 Black tracks (N_b)

These particles have $L < 3$ mm from interaction vertex and $g^* > 6.0$. This corresponds to $\beta < 0.3$ and protons of kinetic energy less than 30 MeV. Most of these are produced due to the evaporation of residual target nucleus. The number of heavily (h) ionizing charged particles (N_h) that are part of the target nucleus is equal to the sum of black and grey fragments ($N_h = N_b + N_g$).

NEDs is a composite target detector and it is composed of mainly H, C, N, O, Ag and Br nuclei. The incident projectile will interact with any one of the targets. These emulsion targets are generally classified into three major classes, which are a combination of Ag/Br nuclei having averaged $A_T = 94$ for heavy; C/N/O nuclei having averaged $A_T = 14$ for medium and the free hydrogen nucleus having $A_T = 1$ for light targets [6,16]. The number of heavily ionizing charged particles depends upon the target breakup. The target separation was achieved by applying restrictions on the number of heavily ionizing charge particles and on residual range of black particles emitted in each event [6,16].

2.4 AgBr target events

N_h value should be equal to or more than 8 and at least one track with $R < 10 \mu\text{m}$ is present in an event.

2.5 CNO target events

N_h value should be in between 2 and 8 and no tracks with $R < 10 \mu\text{m}$ are present in an event. This class always contains very clean interactions of C/N/O target.

2.6 H target events

N_h value should not be greater than one and no tracks with $R < 10 \mu\text{m}$ are present in an event. This class includes not only all $^{84}\text{Kr}+\text{H}$ interactions but also some of the peripheral interactions with C/N/O and the very peripheral interactions with Ag/Br targets.

3. The model

The probability of producing or detecting n number of particles in a pseudorapidity interval $\Delta\eta$ is $P_n(\Delta\eta)$. The probability generating function $Q(\lambda)$ for $P_n(\Delta\eta)$ can be defined as [19]

$$Q(\lambda) = \sum_{n=0}^{\infty} (1 - \lambda)^n P_n(\Delta\eta), \tag{1}$$

where λ is a real variable and is restricted to a suitable convergence domain. $Q(\lambda)$ can be written in terms of the reduced factorial cumulant $\bar{K}_{\bar{N}}$ as

$$Q(\lambda) = \exp \left(\sum_{N=1}^{\infty} \frac{(-\lambda\bar{n})^{\bar{N}}}{N!} \bar{K}_{\bar{N}} \right), \tag{2}$$

where \bar{n} is the average number of particles in the $\Delta\eta$ region. Inverting eq. (1) we have

$$P_n(\Delta\eta) = \frac{(-1)^n}{n!} \left(\frac{\delta^n Q(\lambda)}{\delta \lambda^n} \right)_{\lambda=1}. \tag{3}$$

In order to find the probability of producing zero particles in an interval $\Delta\eta$, we have to substitute $n = 0$ in eq (3):

$$P_0(\Delta\eta) = Q(\lambda)|_{\lambda=1}. \tag{4}$$

Equation (4) depicts the relation between $P_0(\Delta\eta)$ and the generating function $Q(\lambda)$. This probability, $P_0(\Delta\eta)$, in turn, may be used as the generating function for P_n ,

$$P_n(\Delta\eta) = \frac{(-\bar{n})^n}{n!} \left(\frac{\delta}{\delta \bar{n}} \right)^n P_0(\Delta\eta). \tag{5}$$

This equation expresses the relation between n -particle and zero-particle probabilities in a region $\Delta\eta$.

Equation (5) was obtained by allowing only \bar{n} to vary in $P_0(\Delta\eta)$ and all other parameters of $P_0(\Delta\eta)$ are taken to be fixed with respect to variation of \bar{n} . The gap probability also relates probability $P_n(\Delta\eta)$ with $n \neq 0$ through various kinds of moments. $P_0(\Delta\eta)$ can be written as an expansion in cumulants as,

$$\ln P_0(\Delta\eta) = \sum_{N=1}^{\infty} \frac{(-\bar{n})^N}{N!} \bar{K}_N. \tag{6}$$

Applying linked-pair ansatz to normalized cumulant moment K_N [20], we get

$$\bar{K}_N = A_N \bar{K}_2^{N-1}. \tag{7}$$

If linking coefficients A_N are independent of collision energy and pseudorapidity interval and from confirmations of UA1 and UA5 data up to $N = 5$ [20], a quantity called the scaled rap-gap probability χ can be constructed, such that

$$\chi = \frac{-\ln P_0(\Delta\eta)}{\bar{n}}. \tag{8}$$

Then χ depends only on the product of \bar{n} and \bar{K}_2 . This entitles one to write,

$$\chi = \sum_{N=1}^{\infty} \frac{1}{N!} A_N(-\bar{n}\bar{K}_2)^{N-1} = \chi(-\bar{n}\bar{K}_2). \quad (9)$$

Equation (8) shows that for any correlation among particles, the function χ is less than unity. $\chi < 1$ is a direct manifestation of clustering of particles. This feature makes scaled gap probability suitable for investigating the production of charged pions and their structure in rapidity space.

In the clan mode, hadron production in an interaction results from a two-step process. In the first step, hadronic clusters, each of average size \bar{n}_c , are emitted independently from the source, according to a Poisson distribution with average clan multiplicity (\bar{N}). This is followed by a second step by fragmentation of clans into final-state hadrons yielding $\bar{n} = \bar{N}\bar{n}_c$. As clan production is Poissonian, the average clan multiplicity \bar{N} in an interval $\Delta\eta$ is

$$\bar{N} = -\ln P_0(\Delta\eta). \quad (10)$$

The average number of particles per clan is then given by

$$\bar{n}_c = \frac{\bar{n}}{\bar{N}} = \frac{1}{\chi}. \quad (11)$$

The relations (10) and (11) will only be valid when experimentally measured values of χ can be fitted with NB distribution. According to this distribution, linking coefficients increase as $A_N = (N-1)!$ and scaled rap-gap probability χ should satisfy the relation $\chi = \ln(1 + \bar{n}\bar{K}_2)/\bar{n}\bar{K}_2$. This model is called the NB model. If the experimental points of variation of χ against $\bar{n}\bar{K}_2$ can be fitted with the NBD model, $\chi = \ln(1 + \bar{n}\bar{K}_2)/\bar{n}\bar{K}_2$, a scaling behaviour will be observed. In light of this scaling behaviour, we can easily determine the average clan multiplicity \bar{N} and the average number of particles per clan \bar{n}_c in an interval $\Delta\eta$.

4. Results and discussion

The rap-gap probability $P_0(\Delta\eta)$ was calculated for the first pseudorapidity interval ($\Delta\eta = 1$) centred on zero using $^{84}\text{Kr}_{36}$ at ~ 1 A GeV projectiles colliding with heavy (AgBr) and light (CNO) groups of target present in NED. The value of pseudorapidity interval $\Delta\eta$ was then increased in steps of 1 for each interaction and the value of $P_0(\Delta\eta)$ was computed. The values of scaled gap probability for each set of target and projectile were calculated using eq. (8). To calculate single-moment combination ($\bar{n}\bar{K}_2$), we determined the value of \bar{K}_2 . \bar{K}_2 is given by $\bar{K}_2 = (\langle F_2 \rangle - 1)$, where $\langle F_2 \rangle$ is the second-order factorial moment which is given as $\langle F_2 \rangle = \langle n(n-1) \rangle$ and n is the number of particles in the $\Delta\eta$ region.

According to the two-source model, it is assumed that there are two types of sources responsible for the multiparticle production: one is the chaotic source described by the NBD model, while the other is the coherent source described by the minimal model or hierarchical Poisson model [8–11]. If experimental points can be fitted by the NBD model, then multiparticle production mechanism is chaotic. If experimental points can

be fitted with expectations of minimal model, then particle production is coherent [7,8]. However, there is also a possibility that experimental points may lie in the region bounded by the NBD model and the minimal model. Then particle production mechanism is partly coherent and partly chaotic [7–11,21]. The variation of χ with $\bar{n}\bar{K}_2$ is shown in figure 1. The dotted and solid lines represent fitting of the NBD model and the minimal model, respectively. Figure 1 shows that for all interactions, experimental points lie approximately on the dotted curve, suggesting a scaling behaviour.

To confirm the scaling behaviour of the experimental data, we have applied a χ^2 minimization test. The χ^2 per degrees of freedom (χ^2/DOF) of a fit can be obtained by

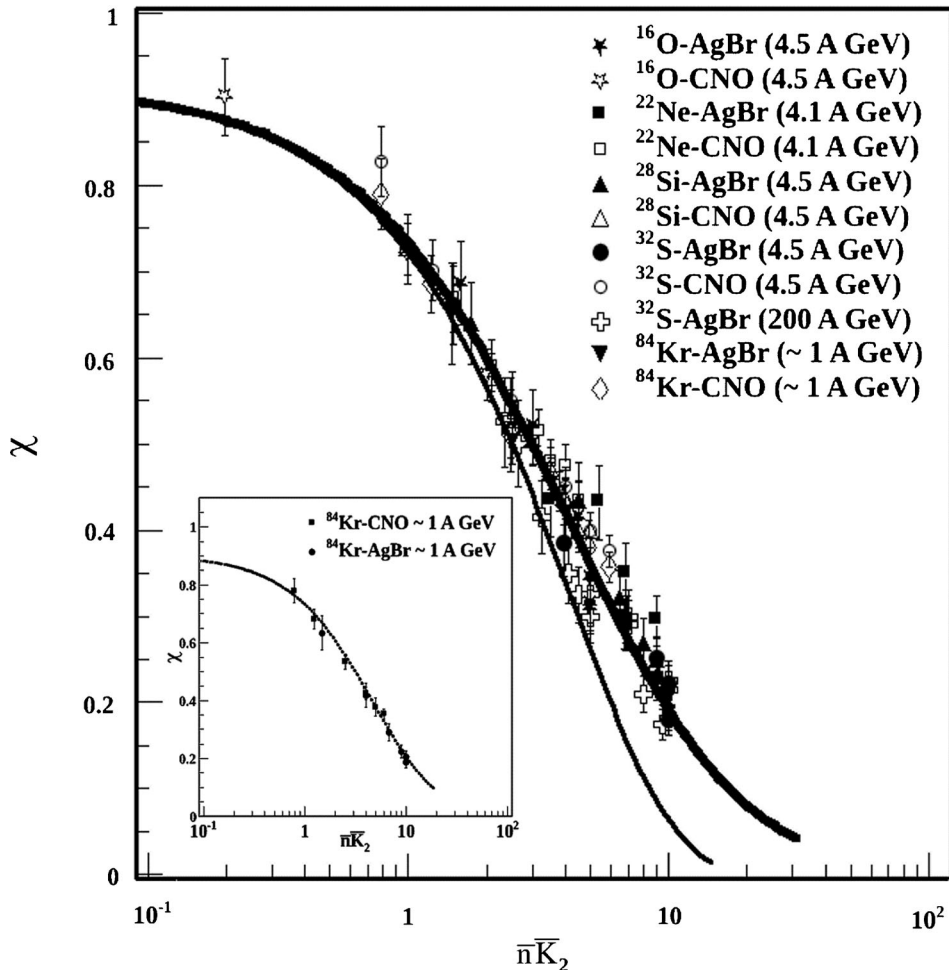


Figure 1. The variation of χ against $\bar{n}\bar{K}_2$. The experimental data points are from ^{16}O at 4.5 GeV/c [5], ^{22}Ne at 4.1 GeV/c [5], ^{28}Si at 4.5 GeV/c [5], ^{32}S at 4.5 GeV/c [5], ^{32}S at 200 GeV/c [6] and ^{84}Kr at 0.95 A GeV. The dotted and solid lines are fitting of data points with the NBD model and minimal model, respectively. For clarity, the present work is separately shown in the inset.

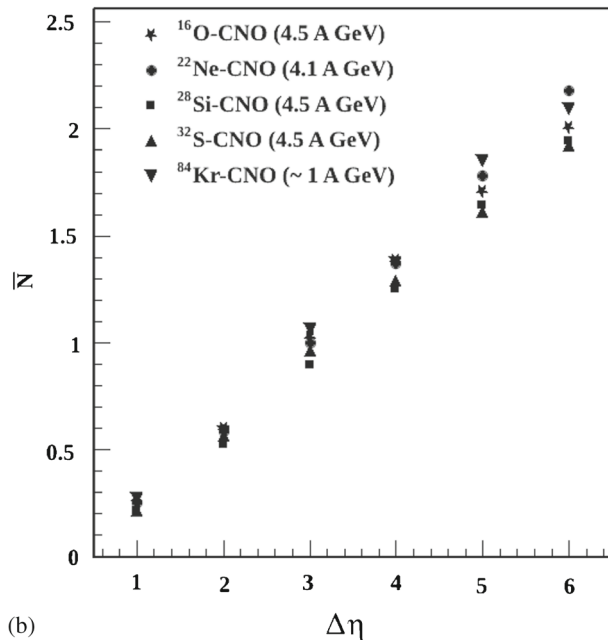
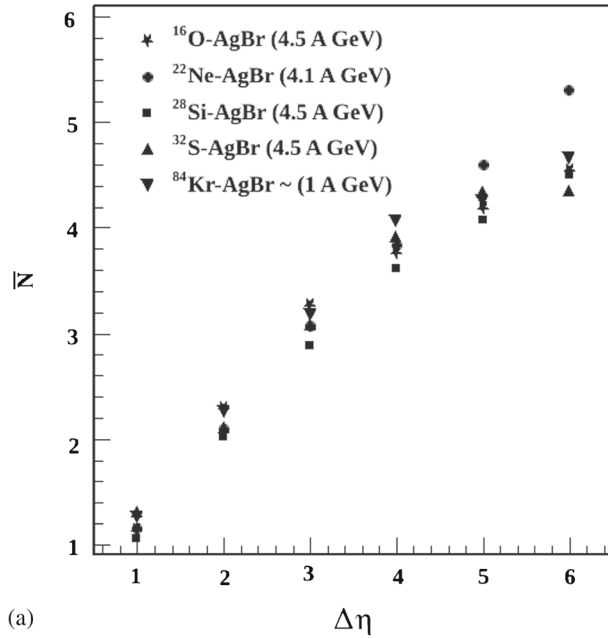


Figure 2. The variation of average clan multiplicity (\bar{N}) against the pseudorapidity interval ($\Delta\eta$) for different projectiles with (a) AgBr target and (b) CNO target.

considering the statistical errors calculated independently of each point, and they form diagonal terms of the full covariance matrix. To have a detailed idea of the full covariance matrix, the correlation between the data points may be taken into account. However,

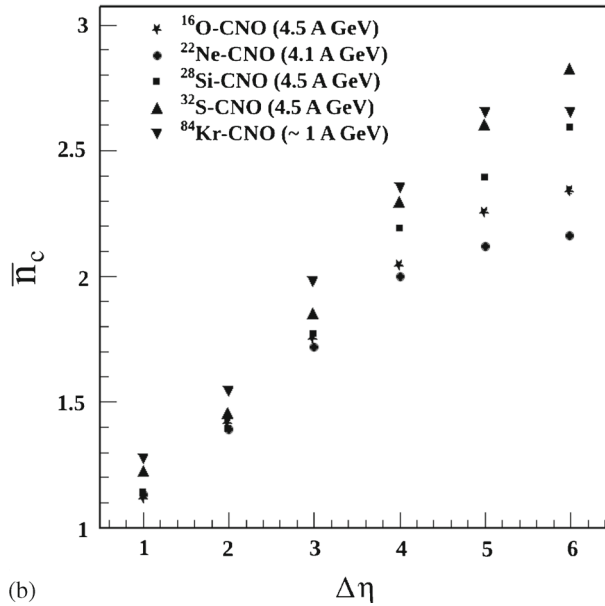
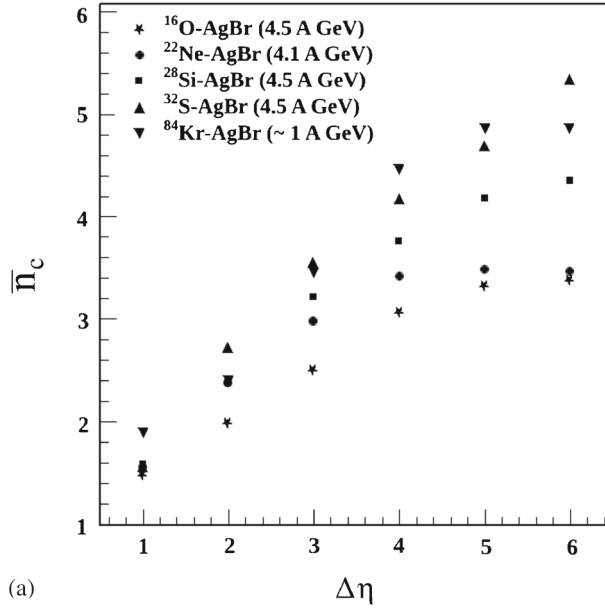


Figure 3. The variation of average number of particles per clan (\bar{n}_c) against pseudorapidity interval ($\Delta\eta$) for different projectiles with (a) AgBr target and (b) CNO target.

several authors reported [7] that although the contributions to the χ^2/DOF values mainly come from the diagonal terms of the full covariance matrix, the changes in the χ^2/DOF values are insignificant when the effects of the off-diagonal terms are taken into account

[7,11]. In the present study we have initially considered the diagonal terms of the full covariance matrix and obtained the χ^2/DOF value of the fit as 0.37. When we consider the off-diagonal terms of the correlation matrix, the χ^2/DOF value of the fit is 0.32. The difference between the values of χ^2/DOF calculated from the full covariance matrix and those calculated from considering the diagonal terms of the covariance matrix is found to be small. The value of χ^2/DOF of the fit is in favour of a good scaling behaviour. This reveals that scaling behaviour of experimental points is explained by the NBD model thus describing pion multiplicity distribution. Therefore, multiparticle production mechanism is chaotic. The experimental points for ^{32}S -AgBr interactions at 200 A GeV lie in the region bounded by the NBD model and the minimal model fitting curves. This observation suggests that particle production at higher energy is partly chaotic and partly coherent. Hence, particle production mechanism is chaotic for low-energy interactions, while it is partly coherent and partly chaotic for higher energy interactions. This inference is also reported by other experimental works [7–11,21–23].

The values of average clan multiplicity in an interval $\Delta\eta$ and the average number of particles per clan (\bar{n}_c) is calculated from eqs (10) and (11). The variation of \bar{N} and \bar{n}_c with $\Delta\eta$ is shown in figures 2 and 3, respectively. The values of average clan multiplicity \bar{N} increase with increase in interval $\Delta\eta$ for both targets, as can be observed from figure 2. The behaviour of average clan multiplicity \bar{N} with interval $\Delta\eta$ is similar for two target groups, while the values of \bar{N} for AgBr target are larger than those for CNO target because the rap-gap probability values of the AgBr target are considerably less than that of the CNO target.

Figure 3 demonstrates that initially there is a systematic increase in the average number of particles per clan (\bar{n}_c) with $\Delta\eta$ for both targets and then saturation of \bar{n}_c is observed for low-mass projectiles (^{16}O and ^{22}Ne) around $\Delta\eta = 6$, while the saturation value of \bar{n}_c increases with increase in projectile size. According to the clan model [13,14], with increase in $\Delta\eta$, more and more D-clans become full clans. The D-clan is a clan that has all or some of its particles in a limited domain D of considered phase space. Hence, \bar{n}_c value is expected to grow, leading to a limiting value. Thus, the saturation value of \bar{n}_c strongly depends on projectile size, which is also reported by other experiments [7–14].

5. Conclusions

The study of clan model parameters and their target dependence in terms of void probability scaling has revealed some interesting physics of multiparticle production process with two different kinds of targets in NED. Depending on the numbers of heavy tracks, total ensembles of events for the projectiles were divided into heavy (AgBr) and light (CNO) groups of target. The variation of scaled rap-gap probability with single moment combination was studied. The experimental scaled rap-gap probability was found to lie approximately on the NBD curve, indicating scaling behaviour. At high-energy interactions, experimental points lie in the region bounded by the NBD model and the minimal model. Therefore, particle production mechanism is chaotic for low-energy interactions and is partly coherent and partly chaotic for higher-energy interactions.

Average clan multiplicity \bar{N} for all interactions increases with increase in pseudo rapidity interval. However, for AgBr target, \bar{N} is higher than that for CNO target. The average

number of particles per clan (\bar{n}_c) initially increases with increase in pseudorapidity interval. The increase in (\bar{n}_c) with $\Delta\eta$ can be explained in terms of the formation of D-clans. It has also been observed from the present analysis that for a particular target, the average number of particles per clan (\bar{n}_c) increases with an increase in the size of the projectile nucleus. Our results are more or less consistent with other experimental works.

Acknowledgement

The authors are grateful to all the technical staff of GSI, Germany, for exposing nuclear emulsion detector with $^{84}\text{Kr}_{36}$ beam.

References

- [1] A Beiser, *Rev. Mod. Phys.* **24**, 273 (1952)
- [2] A Jurak and A Linscheid, *Acta Phys. Pol. B* **8**, 875 (1977)
- [3] D Teaney, J Lauret, Edward and V Shuryak, *Phys. Rev. Lett.* **86**, 4783 (2001)
- [4] N N Abd-Allah and M Mohery, *Turk. J. Phys.* **25**, 109 (2001)
- [5] M K Singh, R Pathak and V Singh, *J. PAS (Phys. Sci.)* **15**, 166 (2009)
- [6] M K Singh, R Pathak and V Singh, *Indian J. Phys.* **84**, 1257 (2010)
- [7] S Bhattacharyya, M Haiduc, A T Neagu and E Firu, *J. Phys. G: Nucl. Part. Phys.* **40**, 025105 (2013)
- N M Agababyan *et al*, *Phys. Lett. B* **382** (1996)
- [8] D Ghosh *et al*, *Phys. Rev. C* **69**, 027901 (2004)
- [9] D Ghosh *et al*, *Phys. Scr.* **77**, 015201 (2008)
- [10] D Ghosh *et al*, *J. Phys. G: Nucl. Part. Phys.* **34**, 2567 (2007)
- [11] D Ghosh *et al*, *J. Phys. G: Nucl. Part. Phys.* **39**, 105101 (2012)
- [12] S Hegyi, *Phys. Lett. B* **274**, 214 (1992)
- [13] A Giovannini *et al*, *Z. Phys. C* **30**, 391 (1986)
- [14] A Giovannini *et al*, *Acta Phys. Pol. B* **19**, 495 (1988)
- [15] M K Singh *et al*, *Indian J. Phys.* **85**, 1523 (2011)
- [16] M K Singh *et al*, *Indian J. Phys.* **87**, 59 (2013)
- [17] M K Singh *et al*, *Indian J. Phys.* **88**, 323 (2014)
- [18] N S Chouhan *et al*, *Indian J. Phys.* **87**, 1263 (2013)
- [19] W Kittel, *Acta Phys. Pol. B* **35**, 2817 (2004)
- [20] P Carruthers *et al*, *Phys. Lett. B* **254**, 258 (1991)
- [21] S Hegyi, *Phys. Lett. B* **274**, 214 (1992)
- [22] D Ghosh *et al*, *Astropart. Phys.* **27**, 127 (2007)
- [23] S Ahmad *et al*, *Fizika B* **16**, 159 (2007)